ELSEVIER

Journal of Membrane Science 125 (1997) 165–175

journal of MEMBRANE SCIENCE

Analysis of the kinetics of vapor absorption/desorption in/from silicone rubber and cellulose acetate membranes in the presence of stagnant boundary layers

D.F. Stamatialis [a,b], M. Wessling [a], M. Sanopoulou [b,*], H. Strathmann [a], J.H. Petropoulos [b]

[a] *Dept. of Chemical Technology, University of Twente, 7500 Enschede, The Netherlands*
[b] *Institute of Physical Chemistry, Demokritos National Research Centre, 15310 Aghia Paraskevi, Athens, Greece*

Received 28 June 1996; revised 12 September 1996; accepted 13 September 1996

Abstract

The application of an interferometric technique (optical thickness meter, OTM) to the measurement of vapor sorption kinetics in both rubbery and glassy polymers is presented. In this technique, the membrane is formed by casting on a suitable glass surface and interferometry is applied in situ. The use of a carrier gas loaded with penetrant vapor introduced a stagnant boundary layer (SBL) effect which had to be corrected, in order to determine true sorption kinetics. The said SBL effect was estimated, on the basis of existing theory for the silicone rubber–methylene chloride (SR/MC) system and found to be more pronounced in the case of desorption. Upon correction for this effect, Fickian sorption curves were obtained; which yielded nearly constant values of the diffusion coefficient, not materially different for absorption and desorption, in line with theoretical expectation.

Cellulose acetate–methylene chloride (CA/MC) was then studied as an example of a glassy polymer–vapor system, where the SBL effect distorts the absorption kinetic curve in the same way as the non-Fickian mechanism of sorption inherent in this kind of polymer–penetrant system. Here, the vapor sorption data were corrected using the results obtained from the Fickian SR/MC system. The corrected results were checked by comparison with independent data reflecting the true kinetic behavior of CA/MC, obtained with a vacuum balance apparatus (VBA), which is free of SBL effects. It is shown that this novel method of applying the SBL correction was reasonably successful in favorable circumstances, while a criterion is provided to identify cases where reasonably reliable correction is not possible.

Keywords: Vapor sorption kinetics; Optical thickness measurements; Concentration polarization; Diffusion; Solubility and partitioning

1. Introduction

Techniques involving measurement of changes in the optical properties of a polymer film exposed to a certain micromolecular penetrant are increasingly being used to study the equilibrium sorption of vapors

* Corresponding author. Fax: +30-1-6511766, Tel.: +30-1-6513111-515, E-mail: sanopoul@cyclades.nrcps.ariadne-t.gr

PII S0376-7388(96)00265-7

or the kinetics of liquid transport in polymeric membranes [1–5].

In the present work we examine the application of an interferometric technique to measure vapor sorption kinetics in both rubbery and glassy polymers with particular emphasis on the latter. The experimental procedure commonly used is to form the polymeric membrane by solvent evaporation on a suitable glass surface and then apply interferometry in situ.

In the experimental set-up used for the interferometric measurements in the present work, the membrane is exposed to a nitrogen stream containing the penetrant vapor. This technique introduces a stagnant boundary layer (SBL) effect and a correction must be made in order to determine true sorption kinetics. This correction can be effected relatively simply, on the basis of existing theory, in the case of a Fickian system with constant diffusion coefficient D; but very little is known about the possibility of applying such corrections to polymer–vapor systems exhibiting more complicated kinetic behavior.

Accordingly, we found it interesting to examine the feasibility of corrections for SBL effects of interferometric kinetic data pertaining to a glassy polymer–penetrant system exhibiting significant concentration dependence of the diffusion coefficient, as well as deviation from normal Fickian kinetics. Cellulose acetate (CA)–methylene chloride (MC) was chosen for this purpose. This work necessitated also study of a simpler system [exemplified by silicone rubber (SR)–MC]; as well as independent data on the true kinetic behavior of CA/MC (obtained with a vacuum balance apparatus; see below) to serve as a check of the results obtained.

It is also noteworthy, that the SBL effects described here, especially during desorption, are of importance in studies of mass transfer dynamics relating to membrane formation. Membrane formation from a polymer–solvent solution cast on an appropriate surface involves evaporation of the solvent from the solution–air interface, solvent diffusion in the solution phase and polymer contraction. Numerous studies, especially in the case of asymmetric membrane formation by phase inversion, are focussed on the evaporation step, which plays an important role not only on the thickness of the dense thin surface layer but also on development of membrane structure and properties [6–9]. Since the evaporation step is usually carried out under free convection conditions, it is obviously subject to important SBL effects.

2. Theory

Fickian diffusion of a penetrant across a thin planar polymer film of dry thickness ℓ_P is described [10,11] by the diffusion equation

$$\frac{\partial C}{\partial t} = \frac{\partial}{\partial x}\left(D\frac{\partial C}{\partial x}\right) \tag{1}$$

where C is the concentration of the sorbed vapor in the membrane (given here in g of vapor per g of dry polymer); D is the diffusion coefficient, which may be constant or a function of C (in a 'polymer fixed' frame of reference); $0 \le x \le \ell_P$ represents the position across the film; and t is the time.

For a sorption experiment the simplest boundary conditions are:

$$C(x, t=0) = C_1 = ka_1; \tag{2a}$$

$$C(x=0, t>0) = C(x=\ell_P, t>0) = C_0 = ka_0 \tag{2b}$$

where a_0, a_1 = const., with $a_0 > a_1$ for absorption and $a_0 < a_1$ for desorption; a is the activity of the vapor (taken here as equal to the relative vapor pressure p/p_{sat}, where p_{sat} is the saturation vapor pressure); and k is the partition coefficient. Under our experimental conditions, $a_1 = 0$ in absorption and $a_0 = 0$ in desorption.

Fickian sorption kinetics in conformity to Eqs. (1) and (2) is described by one of the following equations applicable at short times (semi-infinite membrane condition, which normally remains valid for $M_t/M_\infty \le 0.5$)

$$\frac{M_t}{M_\infty} = 2\sqrt{\frac{D_e t}{\pi \ell_P^2}} \tag{3a}$$

or

$$\frac{M_t}{M_\infty} = 4\sqrt{\frac{D_e t}{\pi \ell_P^2}} \tag{3b}$$

according to whether one or both surfaces of the

membrane are exposed to the vapor, respectively; M_t is the total amount of penetrant sorbed at time t; M_∞ is the amount of penetrant sorbed at the final equilibrium; and the experimental diffusion coefficient D_e is determined from the slope of the linear M_t vs. $\sqrt{t}$ plot. When D is constant, $D_e \equiv D$. When D is a function of C, D_e is a weighted mean value over the range C_l to C_0; if $D(C)$ is an increasing function, $D_e^a > D_e^d$, where the superscripts a and d denote absorption and desorption respectively. At longer times, the M_t vs. $\sqrt{t}$ plot becomes convex upward as $M_t \to M_\infty$. Non-Fickian kinetics on the other hand, is typically characterized by an S-shaped M_t vs. $\sqrt{t}$ plot in absorption, which crosses the corresponding (convex upward) desorption plot.

Eq. (3a) corresponds to the 'optical thickness meter' (OTM) experiments described below, where the membrane adheres to the glass plate (with only one surface exposed to the vapor); while Eq. (3b) applies to the experiments in a high vacuum balance apparatus (VBA), where the polymeric membrane hangs from a quartz spring (with both sides exposed to the vapor).

Eq. (2b) assumes 'perfect agitation' of the vapor reservoir in contact with the membrane surface. In practice, this corresponds to absence of a carrier gas (as in the case of the VBA below). The effect of imperfect agitation of the vapor reservoir (as in the case of the OTM below), is usually represented [12,13] by assuming a stagnant boundary layer (SBL) of thickness ℓ_s adjacent to the exposed membrane surface, whereas the rest of the vapor reservoir is well stirred.

Transport of the penetrant in the SBL is assumed to occur by steady-state diffusion governed by an 'admittance' coefficient α given by [12]

$$\alpha = \frac{D_s}{k\ell_s} \tag{4}$$

where D_s is the diffusion coefficient of the vapor (assumed constant) in the SBL and k is also assumed constant (i.e. α corresponds to the usual mass transfer coefficient divided by the partition coefficient). Efficient stirring corresponds to low values of ℓ_s. The expression for M_t applicable to the $M_t/M_\infty \leq 0.5$ region, when one surface of the membrane is exposed to the vapor (Eq. (3a)) [12] and D = const, is

$$\frac{M_t}{M_\infty} = 2\sqrt{\frac{Dt}{\pi\ell_P^2}} + \frac{D}{\alpha\ell_P}\left[\exp\left(\frac{\alpha^2 t}{D}\right)\operatorname{erfc}\left(\frac{\alpha^2 t}{D}\right)^{1/2} - 1\right] \tag{5}$$

The resulting M_t/M_∞ vs. $\sqrt{t}$ plots are S-shaped. The curvature in the $M_t/M_\infty > 0.5$ range is due (as above) to breakdown of the early-time semi-infinite medium condition, whereas the extent of the curved portion at the low M_t/M_∞ end is determined by the value of

$$B = \frac{\alpha\ell_P}{D} = \frac{D_s\ell_P}{Dk\ell_s} \tag{6}$$

For $B \gg 1$, this portion is small and there remains a substantial middle linear portion described by

$$\frac{M_t}{M_\infty} = 2\sqrt{\frac{Dt}{\pi\ell_P^2}} - \frac{D}{\alpha\ell_P} \tag{7}$$

D may be determined from the slope of Eq. (7). The 'admittance' α then follows from the corresponding intercept on the $\sqrt{t}$ axis

$$\sqrt{t_0} = \frac{1}{2}\frac{\sqrt{\pi D}}{\alpha} \tag{8}$$

Due care must be exercised, however, in the experimental application of Eq. (7). Because of the S shape of the relevant M_t vs. $\sqrt{t}$ plots, it is, in practice, possible to recognize substantial quasilinear middle portions, even where B is quite low and the slope of the said quasilinear portion differs materially from that given by Eq. (7) (cf. Fig. 3 in Ref. [14]). Hence, reasonably efficient agitation to ensure $B \gg 1$ is required. As shown by Eq. (6), this requirement tends to become critical for thin, highly permeable membranes.

No systematic attempt to investigate the applicability of the above treatment under conditions of non-constant D and k has been made; although at least one successful application to a system with k exhibiting significant variability has been reported [13].

3. Experimental

3.1. Materials

Cellulose acetate (CA) powder of 39.8% acetyl content (ca. 2.45 acetyl groups per glucose monomer unit) was supplied by Eastman Chemicals (code name E398-30) with the following specifications: melting range 230–260°C; $T_g = 189$°C; viscosity, [measured according to ASTM D-871 (Formula A) and D-1343] 114 poise (30 s); density, $d_{CA} = 1.31$ g/cm^3 and refractive index, $n_{CA} = 1.4700$, at 25°C.

All the films were prepared by casting a 20% solution of the above powder in acetone (of analytical grade) which was spread with a knife blade on a clean glass surface. After evaporation of most of the solvent, the films for the VBA experiments were taken off the glass plate and solvent evaporation was completed in the open atmosphere and then in vacuo for several days, until the weight of the films became constant. For the experiments in the OTM, the membrane remained on the glass plate and the solvent allowed to evaporate initially in a slow N_2 stream and finally in a vacuum oven at 70°C for several days, until the film thickness measured by the OTM became constant.

Polydimethylsiloxane (silicone rubber, SR) was prepared from a two component rubber, (RTV 615, supplied by General Electric, composed of viscous liquid RTV 615A and crosslinker RTV 615B in the ratio 10:1). Membranes were prepared by casting the above solution on a clean glass plate followed by crosslinking at 70°C for 18 hours. The product was characterised by $T_g = -123$°C; $T_m = -85$°C; density, $d_{SR} = 1.02$ g/cm^3 and refractive index, $n_{SR} = 1.4200$, at 25°C.

Methylene chloride (MC) of analytical grade was used (density, $d_{MC} = 1.32$ g/cm^3 and refractive index, $n_{MC} = 1.4200$, at 25°C).

3.2. Apparatus

3.2.1. Optical thickness meter (OTM)

The OTM (at the University of Twente, supplied by Carl Zeiss, Germany) uses interference of white light in reflection, with incidence at an angle φ (Fig. 1), following a design by Fizeau [15]. Transmission of light from the light source (Halogen lamp, Philips 7027, range 400–1018 nm) to the specimen and of the resulting interference signal from the specimen to the detector is effected by suitable fibre optics. The detector consists of a multichannel spectrometer (MCS 400) which is a polychromator with concave holographic grating and a diode array (512 diodes at a center to center spacing of 0.8 nm). A bus interface is used to connect it with a computer, where the signal is subjected to fast Fourier transformation for the calculation of the optical thickness L given by

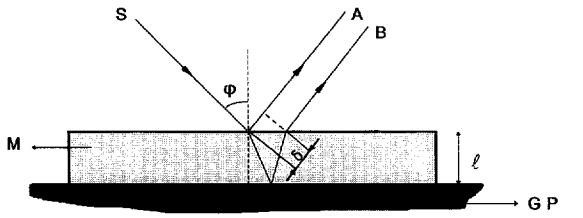

Fig. 1. Interference in reflection from thin films. S: light from source; A, B: light to receiver; M: membrane; GP: glass plate; φ: angle of incidence; δ: path difference (A, B), ℓ: membrane thickness.

$$L = 2\ell\sqrt{n^2 - \sin^2\varphi} \tag{9}$$

In Eq. (9), n is the refractive index and ℓ is the geometrical thickness of the specimen.

In absorption experiments the desired MC vapor activity a_0 was generated by mixing nitrogen with saturated MC vapor at 25°C and atmospheric pressure and passing this mixture at a rate of 1 l/min (controlled by a mass flow controller), through a box thermostatted at 25°C. The latter contained the polymer membrane still lying on the glass casting plate, with its upper surface exposed to the stream. The change of optical thickness of the swelling membrane was measured as a function of time.

In desorption experiments, the boundary condition, $a_0 = 0$, was established by passing pure N_2 through the box.

Thanks to a special design, it was possible to measure the optical thickness of the membrane L and L' at two different angles of incidence, $\varphi = 0°$ and $\varphi = 45°$, respectively. Eq. (9) yields

$$L(\varphi = 0°) = L = 2\ell n \tag{10}$$

$$L(\varphi = 45°) = L' = 2\ell\sqrt{n^2 - 0.5} \tag{11}$$

Using Eqs. (10) and (11), we determined the refractive index and the thickness of the membrane in the dry state (n_P, ℓ_P) and at the end of each absorption experiment (n_∞, ℓ_∞).

Assuming additivity of the refraction per unit volume of the mixture for the components of the mixture, n_∞ can be related to the concentration of the polymer C_P and methylene chloride C_{MC} (in g/cm^3 of mixture) through the Claussius–Mossotti equation [2–4,16]

$$\frac{n_\infty^2 - 1}{n_\infty^2 + 2} = C_{MC} q_{MC} + C_P q_P \tag{12}$$

where q_{MC} and q_P are constants (equal to the molar refraction divided by the molecular weight of MC and the polymer, respectively). Assuming that the polymer on the glass plate does not expand laterally, then

$$C_P = d_P \frac{\ell_P}{\ell_\infty} \tag{13}$$

where d_P is the density of the dry polymer. The constants q_{MC} and q_P are determined by the refractive index and density of the pure substances according to expression $(n^2 - 1)/(n^2 + 2) = qd$. So, the equilibrium absorption isotherms for the systems studied were calculated from Eqs. (12) and (13).

3.2.2. Vacuum balance apparatus (VBA)

The vacuum balance apparatus (at the Democritos Centre) used either a Cahn RG Electrobalance (sensitivity 0.1 μg) or a quartz spring (sensitivity 25.82 cm/g) and has been described in detail elsewhere [17,18]. Absorption and desorption experiments were performed by contacting the evacuated membrane with vapor at activity a_0, and by reevacuating the equilibrated membrane, respectively; while recording the balance reading as a function of time. As previously indicated, these measurements are free of SBL effects.

4. Results and discussion

4.1. Sorption isotherms

The equilibrium data (a) obtained from sorption kinetic experiments with the VBA for the system CA/MC at 25°C and (b) calculated from interference measurements with the OTM [from Eqs. (12) and (13)] for the systems CA/MC [16] and SR/MC at 25°C are presented in Fig. 2.

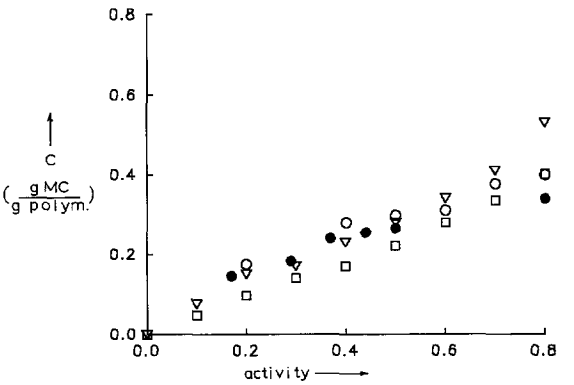

Fig. 2. Absorption isotherm for the systems (a) CA/MC at 25°C from experiments with the (i) VBA, for membrane of thickness 73 μm (▽) and (ii) OTM, for membrane of thicknesses 23.7 μm (○) and 46.65 μm (●) and (b) SR/MC at 25°C from experiments with the OTM for membrane of thickness 38.8 μm (□).

Penetrant activity was not allowed to exceed 0.80 to avoid excessive plasticization and possible loss of integrity of the film (because MC is a strong swelling agent for both CA and SR) and to ensure that the assumption of no significant lateral expansion made for the calculation of the absorption isotherm remains valid. Agreement between the VBA and OTM data was quite satisfactory (particularly in view of the fact that different CA membranes are used).

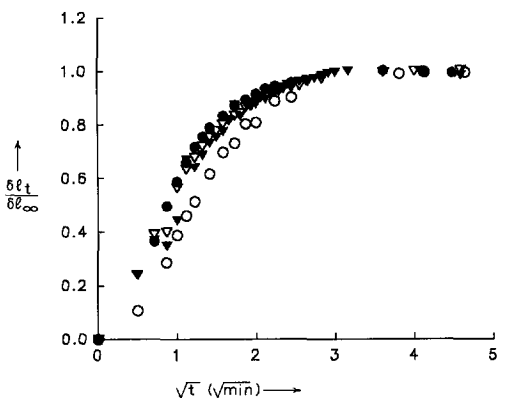

Fig. 3. Fractional thickness kinetic plots for the system SR/MC at 25°C (ℓ_P = 38.8 μm) for absorption experiments, with activity change from $a_1 = 0$ to $a_0 = 0.2$ (○), 0.4 (●), 0.6 (▽), 0.8 (▼).

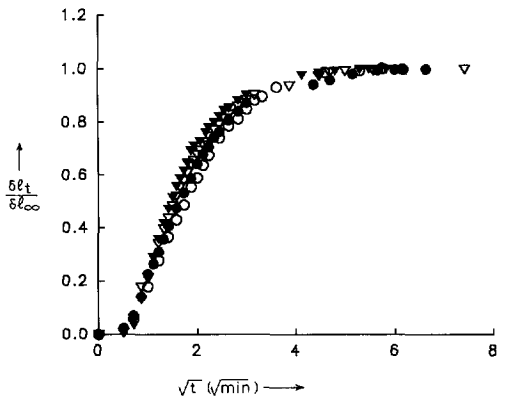

Fig. 4. Fractional thickness kinetic plots for the system SR/MC at 25°C ($\ell_P = 38.8$ μm) for desorption experiments, with activity change from $a_1 = 0.2$ (○), 0.4 (●), 0.6 (▽), 0.8 (▼) to $a_0 = 0$.

Table 1
Evaluation of D and α from OTM data for SR/MC at 25°C

Experiment	a_0	$D_{SR} \times 10^8$ (cm^2/s)	$\sqrt{t_0}$ ($\sqrt{min}$)	$\alpha_{SR} \times 10^5$ (cm/s)	B_{SR}
absorption	0.2	6.41	0.325	8.90	5.41
1st series	0.4	10.65	0.25	14.90	5.45
	0.6	7.50	0.175	17.90	9.29
	0.8	7.39	0.175	17.80	9.35
absorption	0.1	4.73	0.25	10.00	8.18
2nd series	0.3	5.54	0.19	14.40	10.08
	0.5	7.54	0.175	17.90	9.26
	0.7	11.90	0.31	12.60	4.13
desorption	0.2	3.39	0.70	3.00	3.45
	0.4	4.01	0.50	4.60	4.44
	0.6	4.12	0.55	4.20	3.99
	0.8	5.96	0.65	4.30	2.80

4.2. Sorption kinetic curves

4.2.1. SR / MC system

Application of the OTM technique to the system SR/MC at 25°C, yielded diagrams of $\delta L_t/\delta L_\infty$ (which is identical to $\delta\ell_t/\delta\ell_\infty$ because $n_{SR} = n_{MC}$) vs. $\sqrt{t}$ which were S-shaped for all activities of MC (see typical examples in Figs. 3 and 4 for absorption and desorption, respectively). Since Fickian (initially linear) plots are expected for this rubbery polymer, the S-shape is obviously fully attributable to the presence of a substantial SBL, even though the maximum flow rate allowed by the mass flow controller was used throughout to minimise ℓ_s. Accordingly, we proceeded to apply Eq. (7), (with M_t/M_∞ substituted by $\delta\ell_t/\delta\ell_\infty$) to the linear part of the experimental $\delta\ell_t/\delta\ell_\infty$ vs. $\sqrt{t}$ plots (cf. theoretical section).

Diffusion coefficients for absorption and desorption for different boundary activities of MC, at 25°C were calculated from the relevant slopes. The results presented in Fig. 5 showed no significant tendency of the diffusion coefficient to vary with concentration (in contrast to some earlier findings in this respect [19]). From the relevant intercepts $\sqrt{t_0}$, the

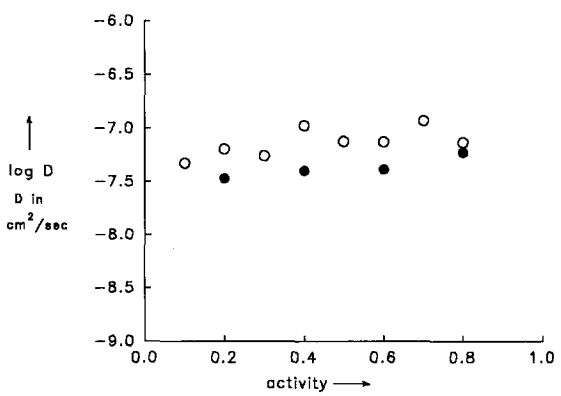

Fig. 5. Diffusion coefficients from absorption (○) and desorption (●) experiments with the OTM for the system SR/MC at 25°C, as a function of MC vapor activity.

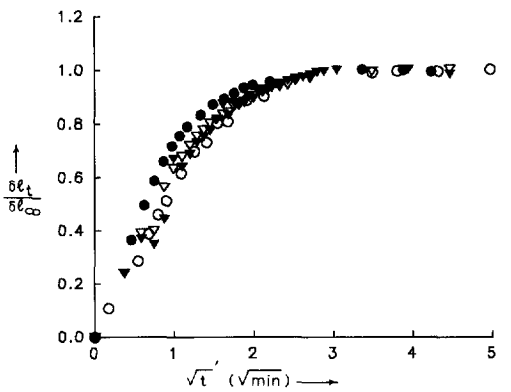

Fig. 6. Corrected fractional thickness kinetic plots ($\delta\ell_t/\delta\ell_\infty$ vs. $\sqrt{t'} = \sqrt{t} - \sqrt{t_0}$) for the system SR/MC at 25°C ($\ell_P = 38.8$ μm) for absorption experiments, with activity change from $a_1 = 0$ to $a_0 = 0.2$ (○), 0.4 (●), 0.6 (▽), 0.8 (▼), (see text).

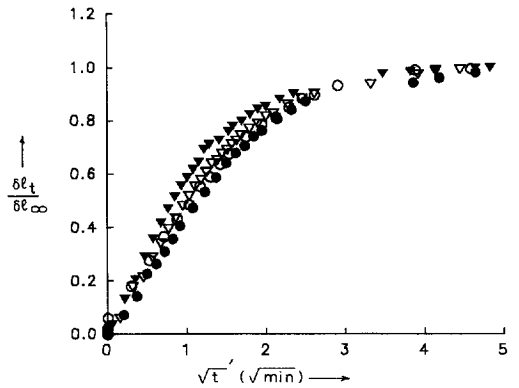

Fig. 7. Corrected fractional thickness kinetic plots ($\delta\ell_t/\delta\ell_\infty$ vs. $\sqrt{t'} = \sqrt{t} - \sqrt{t_0}$) for the system SR/MC at 25°C ($\ell_p = 38.8$ μm) for desorption experiments, with activity change from $a_1 = 0.2$ (○), 0.4 (●), 0.6 (▽), 0.8 (▼) to $a_0 = 0$, (see text).

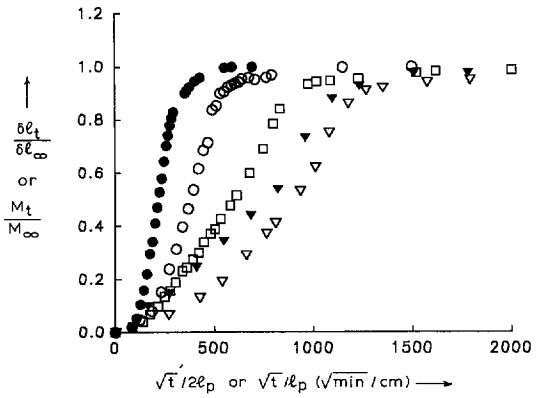

Fig. 8. Absorption kinetics of CA/MC, at 25°C, with $a_1 = 0$, $a_0 = 0.4$. (a) Fractional weight gain (VBA) kinetics (M_t/M_∞ vs. $\sqrt{t}/\ell_p$); membrane thickness: $\ell_p = 37$ μm (▽), 73 μm (▼) or 114 μm (□). (b) Corrected fractional thickness (OTM) kinetics ($\delta\ell_t/\delta\ell_p$ vs. $\sqrt{t'}/2\ell_p$); membrane thickness: $\ell_p = 23.7$ μm (○) or 46.65 μm (●).

coefficients, α_{SR}, and the values of B_{SR} were calculated in each case [from Eqs. (8) and (6) respectively]. The results are presented in Table 1. If the values of $\sqrt{t_0}$ for each experiment (either absorption or desorption) are subtracted from $\sqrt{t}$, the resulting kinetic plots $\delta\ell_t/\delta\ell_\infty$ vs. $\sqrt{t'} = \sqrt{t} - \sqrt{t_0}$ exhibit Fickian behavior as expected (see Figs. 6 and 7).

Table 1 shows, that α_{SR}, as well as B_{SR}, is lower in desorption than in absorption experiments, indicating that the SBL effect is more pronounced in the case of desorption. Moreover from the values of B_{SR} in Table 1, it can be seen that fulfillment of the condition $B \gg 1$ imposed to ensure reliable calculation of D (see theoretical section), is questionable in the case of desorption. This, no doubt, accounts for the fact that the experimental D values shown for desorption (average value: 4.4×10^{-8} cm^2/s) in Fig. 5 are somewhat lower than those for absorption (average value for the 1st and 2nd series of runs: 8.0×10^{-8} cm^2/s and 7.4×10^{-8} cm^2/s, respectively). It appears, therefore, that there is no significant difference in the value of D between absorption and desorption, as expected theoretically in the case of $D = \text{const.}$ (see theoretical section). The above findings confirm ex post facto that the SR/MC system fulfills the most fundamental conditions for reliable estimation of the SBL effect in the OTM, on the basis of the treatment given in the theoretical section and in the light of the findings of Ref. [13].

4.2.2. CA / MC system

For the system CA/MC, the vapor sorption experiments performed with the VBA (which is free from the SBL effect, as already noted) revealed significant concentration dependence of D, as well as typical non-Fickian behavior. In particular (i) the M_t/M_∞ vs. $\sqrt{t}/\ell_p$ plots for absorption were S-shaped and were not coincident for membranes of

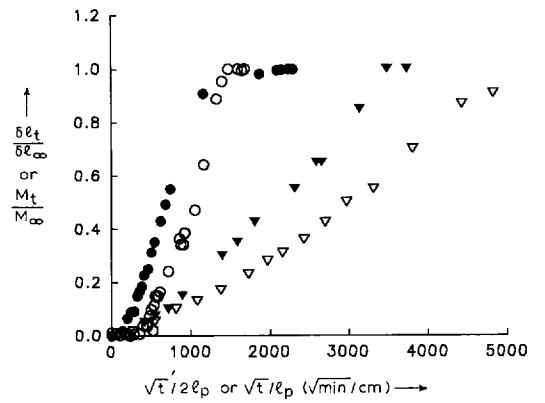

Fig. 9. Absorption kinetics of CA/MC, at 25°C, with $a_1 = 0$, $a_0 = 0.2$. (a) Fractional weight gain (VBA) kinetics (M_t/M_∞ vs. $\sqrt{t}/\ell_p$); membrane thickness: $\ell_p = 37$ μm (▽) and 73 μm (▼). (b) Corrected fractional thickness (OTM) kinetics ($\delta\ell_t/\delta\ell_\infty$ vs. $\sqrt{t'}/2\ell_p$); membrane thickness: $\ell_p = 23.7$ μm (○) or 46.6 μm (●).

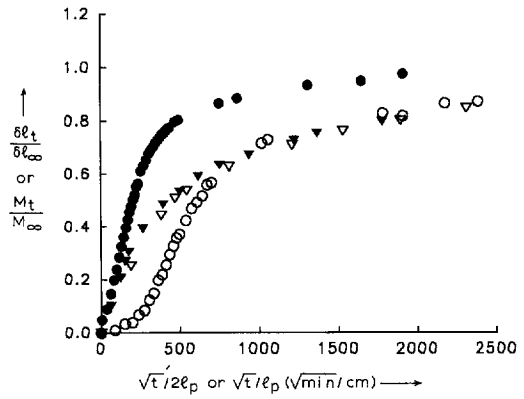

Fig. 10. Desorption kinetics of CA/MC, at 25°C, with $a_1 = 0.4$, $a_0 = 0$. (a) Fractional weight loss (VBA) kinetics (M_t/M_∞ vs. $\sqrt{t}/\ell_p$); membrane thickness: $\ell_p = 37$ μm (▽) or 73 μm (▼). (b) Corrected fractional thickness (OTM) kinetics ($\delta\ell_t/\delta\ell_\infty$ vs. $\sqrt{t'}/2\ell_p$); membrane thickness: $\ell_p = 23.7$ μm (○) or 46.6 μm (●).

different ℓ_p (see examples in Figs. 8 and 9) and (ii) the corresponding desorption plots were not S-shaped (see examples in Fig. 10) and initially lie above, but eventually crossed, the corresponding absorption ones. This behavior can be explained either by molecular relaxation or longitudinal differential swelling stress effects [14,18,20].

In the 0–0.4 activity region studied, the variation in the refractive index of the CA specimens was much smaller than the corresponding changes in thickness (accounting to 0.3% vs. 20% respectively) [16] and $\delta L\ell_t/\delta L_\infty$ did not therefore, differ materially from $\delta\ell_t/\delta\ell_\infty$.

The plots of $\delta\ell_t/\delta\ell_\infty$ vs. $\sqrt{t}$ derived from the OTM were markedly S-shaped for both absorption *and* desorption, due to the presence of the SBL effect. Accordingly, it is interesting to see if agreement between the kinetic behavior shown by the VBA and OTM results can be obtained after correcting the latter for the SBL effect. For this correction, the proper $\sqrt{t_0}$ values must be estimated.

We first note that ℓ_s and D_s should be characteristic constants for the experiments with the OTM at the given N_2–MC stream flow rate. Hence by applying Eq. (4) to both systems (CA/MC and SR/MC) we get:

$$\alpha_{CA} = \frac{\alpha_{SR} k_{SR}}{k_{CA}} \tag{14}$$

Table 2
Evaluation of α for CA/MC OTM curves at 25°C from α for SR/MC and sorption isotherm data

Activity	k_{SR}	$\alpha_{SR} \times 10^5$ (cm/s)	k_{CA}	$\alpha_{CA} \times 10^5$ (cm/s)
0	0.50	4.44	0.85	2.61
0.2	0.45	8.99	0.50	8.05
0.4	0.42	14.90	0.50	12.66
0.5	0.52	17.90	0.55	17.09
0.6	0.55	17.90	0.72	11.62

From Eq. (14) we calculated α_{CA} for each vapor activity of MC presented in Table 2 (the relevant k_{SR} and k_{CA} values were found from the sorption isotherms of each system at activities $a = a_0$ for absorption and $a \cong 0$ for desorption, see Fig. 2). From the linear part of the $\delta\ell_t/\delta\ell_\infty$ vs. $\sqrt{t}$ plots of the system, tentative values of an effective diffusion coefficient D_e were calculated on the basis of Eq. (7). (Model calculations show that meaningful effective D values are, indeed, obtainable in this way if the deviation from Fickian kinetics is not unduly pronounced, cf. Fig. 3 of Ref. [14]).

The resulting tentative values of the parameters $\sqrt{t_0}$ and B_{CA} obtained from Eqs. (8) and (6) respectively, are lower for desorption than for absorption (see Table 3), as in the case of SR/MC and the condition $B \gg 1$ is not satisfied for desorption. The value of $\sqrt{t_0}$ found in each case was used to correct the $\delta\ell_t/\delta\ell_\infty$ vs. $\sqrt{t_0}$ plots of the system. The corrected results together with the M_t/M_∞ results for

Table 3
Estimation of SBL effects in OTM data for CA/MC at 25°C

Experimental conditions	a_0	$\alpha_{CA} \times 10^5$ (cm/s)	$D_{CA} \times 10^8$ (cm²/s)	$\sqrt{t_0}$ ($\sqrt{\text{min}}$)	B_{CA}
$\ell_p = 23.7$ μm	0.2	8.05	0.28	0.08	69.0
Absorption	0.4	12.66	1.88	0.12	16.0
$\ell_p = 46.6$ μm	0.2	8.05	0.41	0.09	90.0
Absorption	0.4	12.66	7.09	0.24	14.0
$\ell_p = 23.7$ μm Desorption	0.4	2.61	0.44	0.29	1.4
$\ell_p = 46.6$ μm Desorption	0.4	2.61	2.24	0.66	5.5

membranes of different thicknesses, at activities $a_0 = 0.4$ and 0.2 are presented in Figs. 8 and 9 respectively. To make the results of these two techniques comparable, the VBA data are presented as M_t/M_∞ vs. $\sqrt{t}/\ell_P$ and the (corrected) ones from the OTM as $\delta\ell_t/\delta\ell_\infty$ vs. $\sqrt{t'}/2\ell_P$. In Fig. 10, similar plots are presented for desorption experiments.

In Figs. 8 and 9 it is shown that, although the same thickness effect is found in both types of experiment, substantially higher absorption rates are exhibited by the membranes used in the OTM compared to the ones used in the VBA. This difference is presumably largely attributable to different pretreatment conditions of formation and after-treatment of the two sets of membranes, as well as different ageing (progressive loss of the in-plane molecular orientation induced by casting on a glass surface) effects in membranes with unconstrained (VBA) or constrained (OTM) longitudinal swelling.

The question of primary importance here is to determine whether OTM data, after correction, can produce the same non Fickian curve shape as the VBA kinetic curves pertaining to membranes of similar thickness, in experiments with the same vapor activity change. For this purpose the kinetic curves shown above were rescaled in time to make them coincide at $\delta\ell_t/\delta\ell_\infty = M_t/M_\infty \cong 0.5$. Examples of this transformation for selected data of Figs. 8 and 10 are presented in Figs. 11 and 12, and Figs. 13 and 14, respectively.

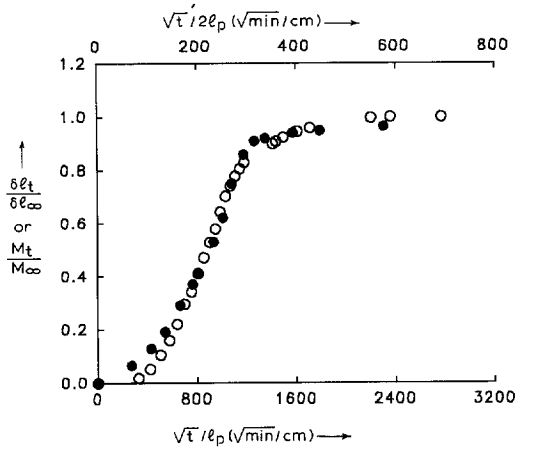

Fig. 12. Comparison of the OTM absorption curve ($\delta\ell_t/\delta\ell_\infty$ vs. $\sqrt{t'}/2\ell_P$) corrected for the SBL effect for the membrane of thickness $\ell_P = 46.6$ μm (○) and the VBA absorption curve (M_t/M_∞ vs. $\sqrt{t}/\ell_P$) for the membrane of thickness $\ell_P = 37$ μm (●), for the system CA/MC at 25°C, with $a_1 = 0$, $a_0 = 0.4$, (see text).

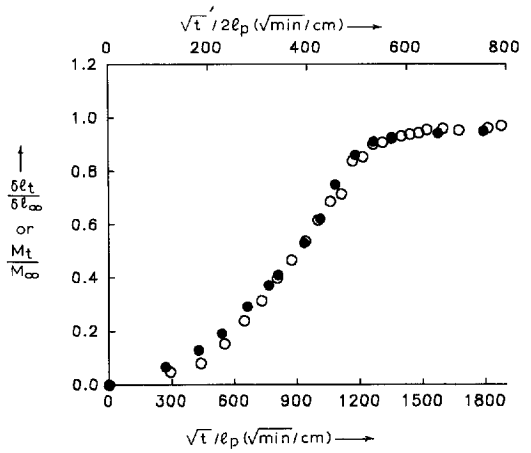

Fig. 11. Comparison of the OTM absorption curve ($\delta\ell_t/\delta\ell_\infty$ vs. $\sqrt{t'}/2\ell_P$) corrected for the SBL effect for the membrane of thickness $\ell_P = 23.7$ μm (○) and the VBA absorption curve (M_t/M_∞ vs. $\sqrt{t}/\ell_P$) for the membrane of thickness $\ell_P = 37$ μm (●), for the system CA/MC at 25°C, with $a_1 = 0$, $a_0 = 0.4$, (see text).

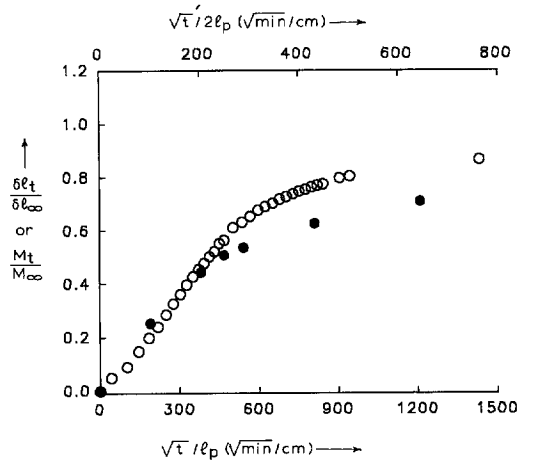

Fig. 13. Comparison of the OTM desorption curve ($\delta\ell_t/\delta\ell_\infty$ vs. $\sqrt{t'}/2\ell_P$) corrected for the SBL effect for the membrane of thickness $\ell_P = 46.6$ μm (○) and the VBA desorption curve (M_t/M_∞ vs. $\sqrt{t}/\ell_P$) for the membrane of thickness $\ell_P = 37$ μm (●), for the system CA/MC at 25°C, with $a_1 = 0.4$, $a_0 = 0$, (see text).

Figs. 11 and 12 show good superposition of the kinetic plots derived from these two different tech-

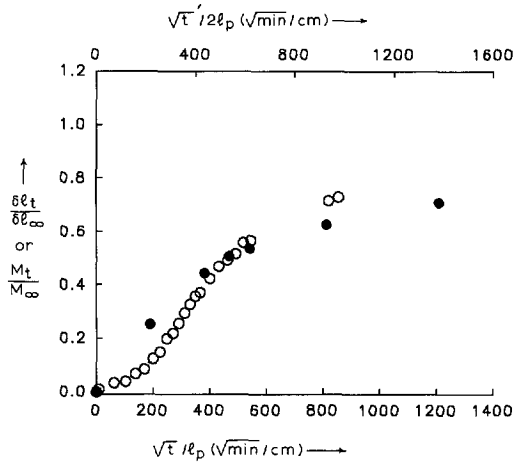

Fig. 14. Comparison of the OTM desorption curve ($\delta\ell_t/\delta\ell_\infty$ vs. $\sqrt{t'}/2\ell_p$) corrected for the SBL effect for the membrane of thickness $\ell_p = 23.7$ μm (○) and the VBA desorption curve (M_t/M_∞ vs. $\sqrt{t}/\ell_p$) for the membrane of thickness $\ell_p = 37$ μm (●), for the system CA/MC at 25°C, with $a_1 = 0.4$, $a_0 = 0$, (see text).

niques for absorption where B_{CA} = 14–90 (see Table 3). This shows that for sufficiently high B_{CA} values, reasonable correction for SBL effects is possible even in systems exhibiting significant concentration dependence of D and deviation from Fickian behavior.

The corresponding data for desorption are shown in Figs. 13 and 14. In this case, as already noted, the

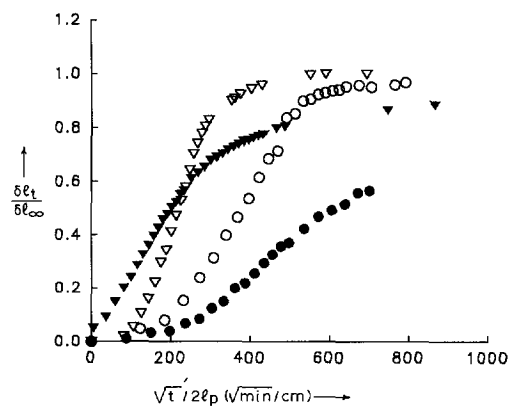

Fig. 15. Relative OTM absorption (open symbols) and desorption (filled symbols) kinetic curves ($\delta\ell_t/\delta\ell_\infty$ vs. $\sqrt{t'}/2\ell_p$) corrected for the SBL effect for the membrane of thickness $\ell_p = 23.7$ μm (○, ●) or 46.6 μm (▽, ▼) for the system CA/MC, at 25°C, with $a_1 = 0$, $a_0 = 0.4$ and $a_1 = 0.4$, $a_0 = 0$, respectively.

estimated B_{CA} values are too low to ensure proper correction, especially for the thin membrane (and, since under these conditions the slope of the quasi-linear part of the kinetic plot yields an underestimate of D, the actual B values must be still lower). Accordingly, it is found that the correction for the SBL effect in the case of the thicker membrane is successful qualitatively, in the sense that the desorption curve is practically not S-shaped and crosses the absorption one (see Fig. 15); but not quantitatively (see Fig. 13). In the case of the thinner membrane, on the other hand, the attempt to correct for the SBL effect fails both quantitatively (see Fig. 14) and qualitatively (see Fig. 15), since the resulting desorption curve is still S-shaped and lies below the absorption one.

5. Conclusion

The main conclusion is that the use of a carrier gas loaded with penetrant vapor in the OTM experimental set up, instead of the vacuum balance system used in conventional sorption experiments, introduces a SBL effect which must be carefully evaluated and corrected in order to avoid errors concerning the interpretation of sorption kinetic curves. This effect was found here to be more pronounced in the case of desorption.

For the SR/MC system, it was shown that the said effect could be estimated reliably on the basis of existing SBL theory, if membranes of appropriate thickness are used. Correction for the estimated SBL effect yielded the expected Fickian sorption curves and D values and behavior, which are reasonable for this kind of system.

In the case of glassy polymers, great care must be exercised, because the stagnant boundary layer affects the absorption curve in the same way as the non Fickian mechanism of sorption inherent in this kind of polymer–penetrant system. The above study of the CA/MC system shows that it is possible to correct glassy polymer–vapor sorption data exhibiting both significant concentration dependence of D and deviation from Fickian behavior, using the results obtained with a simple Fickian system. A criterion is also provided to identify cases where reasonably reliable correction is not possible.

Acknowledgements

European Union support for this work, including a postdoctoral fellowship for D. Stamatialis, within the framework of the Human Capital and Mobility Project entitled 'Functional Membranes', is gratefully acknowledged.

It is a pleasure to dedicate this paper to Dr. Alan S. Michaels in recognition of his far reaching contributions to Membrane Science and Technology in the varied roles of researcher, educator and industrialist, in all of which he excelled.

References

[1] C. Robinson, Interferometric studies in diffusion. I. Determination of concentration distributions, Proc. Roy. Soc. London, A204 (1950) 339.

[2] J.R. Scherer and G.F. Bailey, Water in polymer membranes. Part I. Water sorption and refractive index of cellulose acetate, J. Membrane Sci., 13 (1982) 29.

[3] D.P. Malladi, J.R. Scherer, S. Kint and G.F. Bailey, Water in polymer membranes. Part III. Water sorption and pore volume in cellulose acetate films, J. Membrane Sci., 19 (1984) 209.

[4] B.A. Bolton, S. Kint, G.F. Bailey and J.R. Scherer, Ethanol sorption and partial molar volume in cellulose acetate films, J. Phys. Chem., 90 (1986) 1207.

[5] C.J. Durning, M.M. Hassan, H.M. Tong, and K.W. Lee, A study of Case II transport by Laser interferometry, Macromolecules, 28 (1995) 4234.

[6] C.S. Tsay and A.J. McHugh, Mass transfer dynamics of the evaporation step in membrane formation by phase inversion, J. Membrane Sci., 64 (1991) 81.

[7] W.B. Krantz, R.J. Ray, R.L. Sani and K.J. Gleason, Theoretical study of the transport processes occuring during the evaporation step in asymmetric membrane casting, J. Membrane Sci., 29 (1986) 11.

[8] M. Ataka and K. Sasaki, Gravimetric analysis of membrane casting. I. Cellulose acetate–acetone binary casting solutions, J. Membrane Sci., 11 (1982) 11.

[9] J.E. Anderson and R. Ullman, Mathematical analysis of factors influencing the skin thickness of asymmetric reverse osmosis membranes, J. Appl. Phys., 44 (1973) 4303.

[10] J. Crank, The Mathematics of Diffusion, 2nd edn., Oxford University Press, London, 1975, Chap. 1.

[11] H. Fujita, Diffusion in polymer–diluent systems, Adv. Polym. Sci., 3 (1961) 1.

[12] J. Crank, The Mathematics of Diffusion, 2nd edn., Oxford University Press, London, 1975, Chap. 4.

[13] S.G. Amarantos, K. Papadokostaki and J.H. Petropoulos, Finite bath and boundary layer effects on solute release kinetics from solid matrices, J. Membrane Sci., 34 (1987) 207.

[14] J.H. Petropoulos, Interpretation of anomalous sorption kinetics in polymer–penetrant systems in terms of a time dependent solubility coefficient, J. Polym. Sci., Polym. Phys. Ed., 22 (1984) 1885.

[15] M. Born and E. Wolf, Principles of Optics, Pergamon, New York, 1970.

[16] D.F. Stamatialis, M. Sanopoulou, M. Wessling, H. Strathmann and J.H. Petropoulos, Optical vs. direct sorption and swelling measurements for the study of stiff-chain polymer–penetrant interactions, J. Membrane Sci., submitted.

[17] D.F. Stamatialis, Study of the transport mechanism of micromolecular solvents or swelling agents in glassy polymeric membranes by application of various optical methods, Ph.D. Thesis, University of Athens, 1995.

[18] M. Sanopoulou, P.P. Roussis and J.H. Petropoulos, A detailed study of the viscoelastic nature or vapor sorption and transport in a cellulosic polymer. I Origin and physical implications of deviations from Fickian sorption kinetics, J. Polym. Sci., Polym. Phys. Ed., 33 (1995) 993.

[19] I. Blume, P.J.F. Schwering, M.H.V. Mulder and C.A. Smolders, Vapor sorption and permeation properties of poly(dimethylsiloxane) films, J. Membrane Sci., 61 (1991) 85.

[20] M. Sanopoulou, P.P. Roussis and J.H. Petropoulos, A detailed study of the viscoelastic nature or vapor sorption and transport in a cellulosic polymer. II. Sorption and longitudinal swelling kinetic corrections, J. Polym. Sci., Polym. Phys. Ed., 33 (1995) 2125.